

Stabilization of zero-energy skin modes in finite non-Hermitian lattices

C. Yuce  and H. Ramezani 

*Department of Physics, Eskisehir Technical University, Eskisehir, Turkey
and Department of Physics and Astronomy, University of Texas Rio Grande Valley, Edinburg, Texas 78539, USA*



(Received 31 May 2022; accepted 8 November 2022; published 2 December 2022)

The zero energy of a one-dimensional semi-infinite non-Hermitian lattice with nontrivial spectral topology may disappear when we introduce boundaries to the system. While the corresponding zero-energy state can be considered as a quasi-edge state for the finite lattice with a long survival time, any small disruption (noise) in the initial form of the quasi-edge state can significantly shorten the survival time. Here, by tailoring the couplings at one edge we form an exceptional point allowing for a topological phase transition and the stabilization of the quasi-edge state in a finite-size lattice with open edges. Such a small modification in the lattice does not require closing and opening of the band gap and opens the door for experimental realization of such robust zero-energy edge states.

DOI: [10.1103/PhysRevA.106.063501](https://doi.org/10.1103/PhysRevA.106.063501)

I. INTRODUCTION

The energy bands of non-Hermitian Hamiltonians can exhibit unique nontrivial topological features characterized by the spectral winding number [1]. In sharp contrast to Hermitian systems, even a single-band non-Hermitian system without any symmetry restrictions can be topologically nontrivial when its spectrum under the periodic boundary conditions (PBC) forms a loop or loops in the complex energy plane. Remarkably, the spectrum of such a system is highly sensitive to boundary conditions [2–31]. A topological phase transition occurs when we introduce boundaries and the system under open boundary conditions (OBCs) becomes topologically trivial in terms of a point gap [32–35]. This leads to the failure of the conventional bulk boundary correspondence, as well as to the emergence of the non-Hermitian skin effect; i.e., eigenstates that are not at the Bloch points are localized at the edge under OBCs [36,37]. Fortunately, a bulk boundary correspondence can be established by considering the semi-infinite boundary conditions (SIBCs), which assume a boundary on the left but no boundary on the right. Its spectrum fills the interior of the loop formed by the PBC spectrum in the complex energy plane [32]. An infinite number of skin states inside the loop emerge as a result of the nontrivial spectral winding number. We note that the spectrum under OBCs is a subset of the spectrum under SIBCs for such systems. A skin state whose energy is not in the OBC spectrum is a mathematical solution as any experiment contains a finite number of lattice sites. Nevertheless, it can be used in the finite lattices as a quasi-edge state that is not an eigenstate but acts as if it is an eigenstate up to a survival time, which increases with system size [38,39]. It was shown that quasi-edge modes can survive at the interface between two topologically distinct nonreciprocal finite lattices after judicious tailoring of the complex on-site potentials at the edges of a finite-size topological interface [40].

In this paper, we consider single-band and two-band chiral-symmetric one-dimensional (1D) non-Hermitian tight-binding lattices with asymmetric couplings. We first explore survival times for quasi-edge states in finite lattices with open edges. We show that survival time increases with the system size and then saturates due to their fragility against noise. We see that even the numerical rounding errors for finding survival time may lead to huge fluctuations at large times in a long lattice. We secondly show that stabilization of the quasi-edge state in the finite lattices can also be possible by judiciously changing the coupling at one edge of the system. Recently, it has been discussed that a quasi-edge mode among the infinitely many ones can be selectively stabilized in a finite single-band non-Hermitian lattice provided that on-site potentials are judiciously introduced to the system [41]. However, such a change breaks the chiral symmetry. We propose to judiciously change the coupling at the edge not to break the chiral symmetry for the stabilization of the quasi-edge zero-energy state. We show that a zero-energy topological state appears in the middle of the band gap with a perturbative change of the coupling. In this way, we are also able to change the topological phase of the system by generating an exceptional point in some finite two-band models.

II. SINGLE-BAND MODEL

Skin states can appear under SIBCs or OBCs due to the non-Hermitian skin effect. We note that an OBC skin state is also a SIBC skin state, but the reverse is not always true. A quasi-edge state is a skin state at an energy E in a finite lattice with OBCs whose spectrum does not include E . An exactly solvable model helps us better understand the survival times and stabilizations of the quasi-edge states. We start with the Hatano-Nelson model describing a one-dimensional tight-binding lattice with asymmetric couplings between adjacent

sites [42]:

$$J_L \Psi_{n+1} + J_R \Psi_{n-1} = i \frac{d\Psi_n}{dt}, \quad (1)$$

where J_R and J_L are the couplings in the forward and backward directions, respectively; $n = 1, 2, \dots, N$; and Ψ_n is the time-dependent field amplitude at the n th lattice site. Note that we mathematically suppose $\Psi_0 = 0$ for the system with an open edge on the left. The other conditions for the OBC and the SIBC read $\Psi_{N+1} = 0$ and $\Psi_\infty = 0$, respectively. A simple analytical solution is available for the system with unidirectional couplings $J_L = 1$ and $J_R = 0$. The eigenfunctions ($\Psi_n = e^{-iEt} \psi_n$) subject to the PBC ($\psi_{n+N} = \psi_n$), OBC, and SIBC are given by

$$\begin{aligned} \psi_n^{(\text{PBC})} &= e^{ikn}, \\ \psi_n^{(\text{OBC})} &= \delta_{n,1}, \\ \psi_n^{(\text{SIBC})} &= e^{(-\kappa+ik)(n-1)}, \end{aligned} \quad (2)$$

with corresponding eigenvalues $E_{\text{PBC}} = e^{ik}$, $E_{\text{OBC}} = 0$, and $E_{\text{SIBC}} = e^{-\kappa+ik}$, where $\kappa > 0$ and $-\pi < k < \pi$. Note that all nonzero eigenvalues come in pairs $(-E, E)$ due to the chiral symmetry, and an exceptional degeneracy occurs at zero energy. The PBC spectrum describes a circle with a unit radius in the complex plane and the SIBC spectrum fills the interior of this circle. On the other hand, an exceptional point occurs under the OBC and all eigenstates coalesce to a single eigenstate for any finite value of N . The PBC states are extended, whereas the OBC and SIBC states are localized skin states. In this specific example, the quasi-edge states are the SIBC skin states with nonzero eigenvalues. Recall that quasi-edge states are the states that are the eigenstates under SIBCs but not OBCs, so they are just mathematical solutions as any experiment contains a finite number of lattice sites. Nevertheless, if a quasi-edge state is initially prepared in a finite lattice with open edges, then it almost keeps its spatial form up to a survival time τ . To see this analytically, we write the general solution of Eq. (1) at $J_L = 1$ and $J_R = 0$ under the OBC as

$$\Psi_n(t) = \sum_{j=0}^{N-n} c_{n+j} \frac{(-it)^j}{j!}, \quad (3)$$

where c_n is determined by the initial wave packet. The field amplitude is constant at the right edge ($\Psi_N(t) = c_N$) and time dependent at all other sites, causing a localized wave packet to eventually lose its form. The growth is more rapid in the far left of the lattice, so the total power becomes mostly concentrated at the left edge at sufficiently large times independent of the form of the initial wave packet. Fortunately, if a skin state $\psi_n^{(\text{SIBC})}$ with energy $E \neq 0$ is initially prepared in a finite lattice, then it stays almost stationary up to a survival time τ [$\Psi_n(t) \approx e^{-iEt} \psi_n^{(\text{SIBC})}$] and then the wave packet deforms rapidly starting from the left edge. Therefore, the ratio $\frac{\Psi_1(t)}{\Psi_1(0)}$ helps us roughly determine τ . Using Eq. (3) and the relation $\Gamma(N, t) = \Gamma(N) e^{-t} \sum_{j=0}^{N-1} \frac{t^j}{j!}$, we get

$$\frac{\Psi_1(t)}{\Psi_1(0)} = e^{-i\alpha t} \frac{\Gamma(N, -i\alpha t)}{\Gamma(N)}, \quad (4)$$

where $\alpha = e^{-\kappa+ik}$ and $\Gamma(N)$ and $\Gamma(N, t)$ are complete and incomplete gamma functions, respectively. This ratio is almost equal to 1 when $0 < t < \tau$ and then rapidly grows. We can determine τ at which this ratio changes, for example, one percent from its initial value. We numerically see that the survival time τ increases linearly with N [38]. However, an observation of this linear dependence ($\tau \propto N$) is practically impossible at large values of N since a system with a larger value of N is more sensitive to the unavoidable noises in the preparation of the system in a pure quasi-edge state. Consider, for example, a perturbation to the initial wave packet such as $\Psi_n(t=0) = (1 + \epsilon W_n) \psi_n^{(\text{SIBC})}$, where W_n are random numbers in the interval $[0, 1]$ and $\epsilon \ll 1$. At $N = 100$, $\kappa = 1$, $k = 0$, and $\epsilon = 0$, we numerically find $\tau \approx 90$, which is a typical timescale in non-Hermitian systems with waveguides [43], but it is reduced dramatically from 90 to 30 even for a tiny value of $\epsilon = 10^{-5}$. This gets worse for a larger value of N , which implies that one can numerically see a saturated value of τ (it does not increase linearly indefinitely with N) since even the rounding errors in numerical computations become large enough to produce a rapid distortion of the quasi-edge state.

We can stabilize a particular quasi-edge state for a finite lattice by a proper perturbative change of the coupling; i.e., we make $\tau \rightarrow \infty$ for a particular state among infinitely many ones. We pick the quasi-edge state at energy $E_c \neq 0$ (2). To stabilize it in a finite lattice with open edges, we judiciously change only the forward coupling at the right edge of the unidirectional lattice, which is a perturbative change ($N \gg 1$): $J_L = 1$ and $J_R = E_c^2 \delta_{n,N}$. In this case, the eigenvalues become 0 and $\mp E_c$ and the target quasi-edge state $\psi_n^{(\text{SIBC})}(E = E_c)$ becomes an eigenstate of the finite lattice. Note that the chiral symmetry is not broken with this coupling change and hence not only the quasi-edge state with energy E_c but also the one with energy $-E_c$ is stabilized in the finite lattice. As a result, we analytically see how a perturbative change can lead to a nonperturbative change on the spectrum. This approach has a more intriguing result for some chiral symmetric two-band models in which the zero-energy quasi-edge state in particular is stabilized. Such a stabilization by a perturbative change in the Hamiltonian leads to the formation of an exceptional point. Therefore, we can change a topologically trivial system into a nontrivial one just by a perturbative change of the coupling at the right edge as we see below.

III. TWO-BAND MODEL

A non-Hermitian Hamiltonian can have two different types of topological modes [33,34]: the conventional topology that can be described by the bulk topological invariants based on the non-Bloch band theory [44] and the spectral topology that can be characterized by the spectral winding number at a complex base energy E_B , $w(E_B) = \frac{1}{2\pi i} \int_{-\pi}^{\pi} dk \partial_k \ln(E_k - E_B)$ [1]. Below, we consider both types of topological modes in some two-band models.

Consider a one-dimensional tight-binding lattice with two sites per unit cell and asymmetric couplings in forward and backward directions between adjacent sites. Figure 1 depicts three such systems. Let us first discuss their common features and then study each system separately. The corresponding

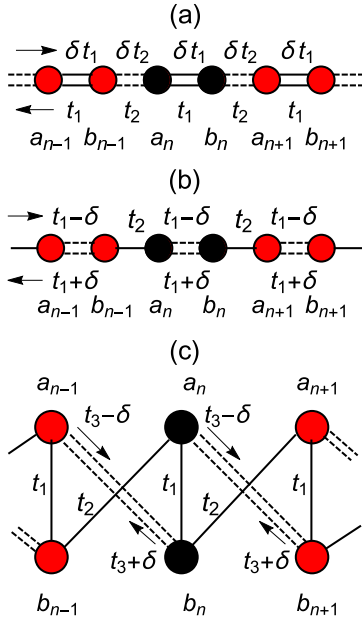


FIG. 1. Three different one-dimensional tight-binding lattices with two sites per unit cell, where a_n and b_n are the field amplitudes in the n th sublattices. The couplings represented by double lines between adjacent sites are nonreciprocal.

2×2 Bloch Hamiltonian in k -space for each of these systems has the form ($-\pi < k < \pi$)

$$\mathcal{H} = \begin{pmatrix} 0 & d_x - id_y \\ d_x + id_y & 0 \end{pmatrix}, \quad (5)$$

where d_x and d_y are k -dependent complex functions to be determined specifically for each system. The above Bloch Hamiltonian has a chiral symmetry, $\sigma_z \mathcal{H} = -\mathcal{H} \sigma_z$, which means that the energy spectrum is symmetric with respect to zero energy. We can readily write the PBC spectrum, which forms a loop or loops in a complex energy plane as k varies over the first Brillouin zone:

$$E_{\text{PBC}} = \mp \sqrt{d_x^2 + d_y^2}. \quad (6)$$

This expression fails to predict the OBC energy spectrum. The dramatic difference between the PBC and OBC spectra can be interpreted as the source of the so-called non-Hermitian skin effect, implying that the standard bulk boundary correspondence is broken.

The number of skin states at a particular complex base energy E_B inside the PBC loop is equal to $|w(E_B)|$. Of special importance is the zero-energy skin state. Suppose that $|w(E_B = 0)| = 1$ (the zero-energy point is encircled by the PBC loop in the complex plane). This means that there must exist only one skin state at zero energy, $E_B = 0$. On the other hand, the chiral symmetry causes the energy eigenvalues to be symmetric ($-E, E$). Therefore, a second-order exceptional point necessarily appears under the OBC provided that the OBC spectrum contains zero energy. In the conventional sense, this is a topological zero-energy state [36,37,44].

Suppose now that the OBC spectrum does not contain zero energy,; i.e., the system is topologically trivial in the conventional sense. We further suppose that a zero-energy

state is available under the SIBC. That state can nevertheless be used as a quasi-edge state in the finite lattice with open edges. Below, we specifically consider the three models in Fig. 1 and compute the survival times of the zero-energy quasi-edge states. Unfortunately, the quasi-edge modes are highly sensitive to noise and this limits their experimental observations. Therefore, we aim at stabilizing them through some perturbative changes in the coupling at the edge. We can, in principle, stabilize the quasi-edge state at any energy but we are here particularly interested in the zero-energy quasi-edge state. Remarkably, picking it out of the infinite number of quasi-edge states has another interesting effect in addition to its stabilization. This also generates an exceptional point in the finite lattice under the OBC and hence turns the conventional topological phase of the system from trivial to nontrivial by a perturbative change in the Hamiltonian. This is unique to the non-Hermitian system as it is not predicted by the standard bulk-boundary correspondence, which requires band gap closing and reopening for the topological phase transition. Let us illustrate our discussions on the three models in Fig. 1.

1. Model I

We start with the first model depicted in Fig. 1(a), where a_n and b_n are field amplitudes at the n th unit cell. This model is a tight-binding lattice with asymmetrical and staggering couplings between adjacent sites. The corresponding Hamiltonian in k -space reads

$$\mathcal{H} = \begin{pmatrix} 0 & t_1 + \delta t_2 e^{-ik} \\ \delta t_1 + t_2 e^{ik} & 0 \end{pmatrix}, \quad (7)$$

where t_1 and t_2 are positive staggering couplings in the backward direction and $0 < \delta < 1$ is the multiplicative factor for the couplings in the forward direction.

The OBC spectrum is gapped and lies along the real axis when $t_1 > t_2$, whereas the corresponding PBC spectrum describes a closed loop in the complex plane as depicted in Fig. 2(a). Decreasing t_1 at fixed t_2 and δ will reduce the OBC band-gap width until the band gap closes at $t_1 = t_2$. If we further decrease the coupling t_1 ($t_1 < t_2$), the OBC spectrum becomes gapped again and a zero-energy state appears in the middle of the band gap. This zero-energy state is, in fact, the conventional topological zero-energy mode in the finite lattice. On the other hand, the semi-infinite lattice can have a zero-energy skin mode over a wider range of the parameters as can be seen from the exact zero-energy solution of the corresponding eigenvalue equation subject to the SIBC ($a_\infty \rightarrow 0$ and $b_\infty \rightarrow 0$):

$$a_n = \left(\frac{-\delta t_1}{t_2} \right)^n, \quad b_n = 0, \quad (8)$$

which shows that the zero-energy mode is available under the SIBC as long as $\delta \times t_1 < t_2$. At the critical point $\delta \times t_1 = t_2$, this zero-energy solution no longer satisfies the SIBC while it satisfies the PBC, indicating the formation of an exceptional point under the PBC. For $\delta \times t_1 > t_2$, no zero-energy skin mode appears in the semi-infinite lattice and the PBC spectrum does not encircle the zero energy but makes two separate loops excluding the zero energy.

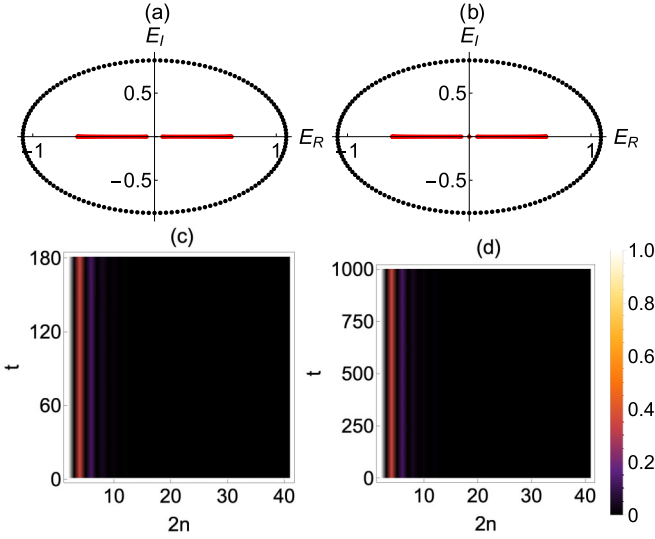


FIG. 2. The PBC (in black) and OBC (in red) energy spectra in the complex plane at $t_1 = 1.1$, $t_2 = 0.9$, $\delta = 0.1$, and $N = 100$ for model I (a) and stabilized model I (b). The latter one has a conventional topological zero-energy mode under the OBC, while the former one does not. The absolute values of the field amplitudes as a function of time for the zero-energy quasi-edge state [panels (c) and (d)] corresponding to the system in panels (a) and (b), respectively. For clarity, only the portion up to $2n = 40$ is shown. The form of the initial wave packet remains almost the same until $t \approx 180$ for panel (c) while it is truly stable for panel (d).

Consider now that $\delta \times t_1 < t_2$ and $t_1 > t_2$, at which the SIBC spectrum contains zero energy but the OBC spectrum does not. This means that the truncated zero-energy SIBC state can be used as a quasi-edge state for the finite lattice with open edges. We next find its survival time. Suppose that we prepare an initial wave packet according to Eq. (8) for $n = 1, 2, \dots, N$. This initial wave packet is not an exact stationary state for the finite lattice but can still be used as a quasistationary solution since $a_{N+1} \ll a_1$. We then numerically compute its time evolution for the parameters given in Fig. 2(a) and $N = 100$. The survival time τ at which the wave packet starts to lose its initial form is quite long as is shown in Fig. 2(c). However, similar to the previously studied case of the single-band model, τ reduces considerably in the presence of noise on the initial wave.

Let us next stabilize the zero-energy quasi-edge state as it also enables us to change the topological feature of the finite system. As mentioned in the preceding section, we can judiciously change the coupling at the right edge for stabilization. Therefore, we assume that the coupling in the forward direction at the edge is zero instead of δt_2 as shown in Fig. 3(a). This is a perturbative change since all other couplings along the lattice with $N \gg 1$ remain intact. With this perturbative change, a second-order exceptional point is necessarily formed and hence a conventional topological zero-energy state localized at the left edge appears in the middle of the band gap [see Fig. 2(b)]. We stress that chiral symmetry, given by the chiral operator \mathcal{C} as the diagonal matrix with elements $C_{nm} = (-1)^n \delta_{n,m}$, is not lost under this perturbative change and the energy eigenvalues stay symmetric with zero

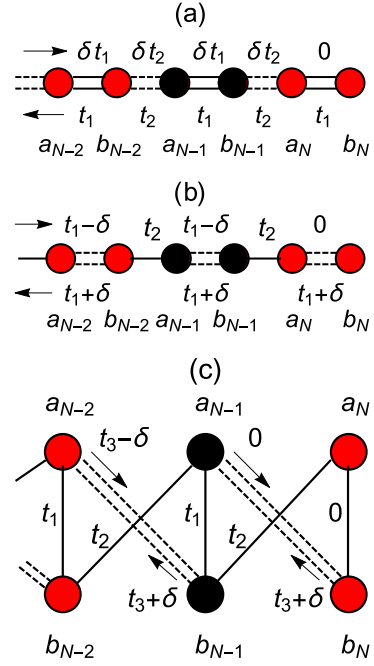


FIG. 3. The couplings at the edge are changed for the three models shown in Fig. 1 to stabilize the zero-energy quasi-edge state. An exceptional point at zero energy is necessarily formed and a topological zero-energy mode appears in the finite lattice with open edges after such a change of the couplings.

energy. As a final step, we plot the corresponding density for the zero-energy state in this finite lattice in Fig. 2(d) up to $t = 1000$, which shows its stationary character.

We conclude that the stabilization of the zero-energy quasi-edge state is possible by generating an exceptional point. In this way, the topological feature of the finite system with open edges is also changed. According to the standard theory of Hermitian topological insulators, a topological phase transition in one dimension can happen with a band gap closing and reopening. However, this is not the case in our system and a topological phase transition occurs through a perturbative change in the system without the band gap closing. Furthermore, the zero energy topological modes in Hermitian systems are robust against a symmetry-protecting disorder unless the disorder strength is strong enough to close the band gap. In the above non-Hermitian system, they are robust against a chiral symmetry-protecting disorder as long as the exceptional point is not lost.

2. Model II

Let us now consider another configuration depicted in Fig. 1(b) [37]. This system has asymmetric intradimer couplings $t_1 \mp \delta$ and symmetric interdimer couplings t_2 , where t_1 , t_2 , and δ are all positive constants with $\delta < t_1$. The Hamiltonian for the system is given by Eq. (5) with

$$d_x = t_1 + t_2 \cos k, \quad d_y = t_2 \sin k + i\delta. \quad (9)$$

The corresponding PBC spectrum can be found using Eq. (6). An exceptional point at the band edge occurs at $t_1 = t_2 \mp \delta$ (or $t_1 = -t_2 \mp \delta$ at the band center). Beyond this point, the PBC spectrum makes two separate loops excluding

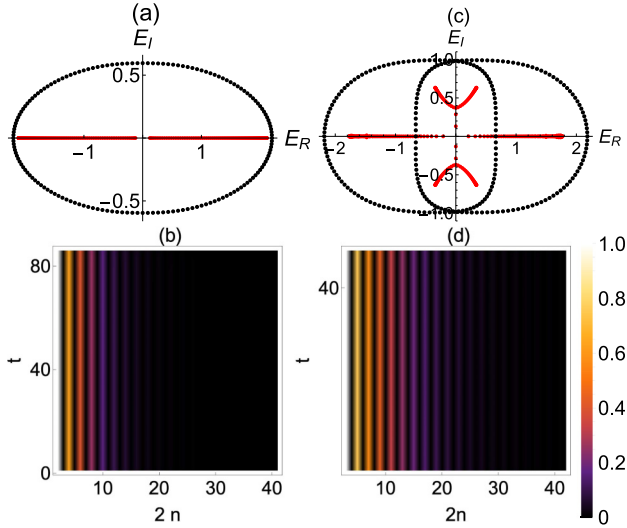


FIG. 4. The PBC (in black) and OBC (in red) at $N = 100$ spectra for model II (a) and model III (c). The density plot $|\psi_n|$ for the zero-energy quasi-edge state as a function of time for model II (b) and model III (d). The plots are up to $2n = 40$ for clarity. The parameters are $t_1 = 1.3$, $t_2 = 1$, and $\delta = 2/3$ for model II and $t_1 = 0.6$, $t_2 = 0.8$, and $t_3 = \delta = 1$ for model III.

the zero-energy point. On the other hand, the corresponding OBC spectrum can be derived using the non-Bloch band theory [45]: $E_{\text{OBC}}^2 = t_1^2 + t_2^2 - \delta^2 + 2t_2\sqrt{t_1^2 - \delta^2} \cos \theta$ for $|\delta| < t_1$ and $E_{\text{OBC}}^2 = t_1^2 + t_2^2 - \delta^2 - 2it_2\sqrt{\delta^2 - t_1^2} \sin \theta$ for $|\delta| > t_1$, where $-\pi < \theta < \pi$. These expressions indicate that the OBC spectrum is real when $|\delta| < t_1$ and the topological zero-energy modes are available when $t_2^2 \geq t_1^2 - \delta^2$ [37]. As an example, the PBC and OBC spectra can be seen in Fig. 4(a) for $t_1 = 1.3$, $t_2 = 1$, and $\delta = 2/3$.

Let us now analytically solve the corresponding eigenvalue equation to find the exact form of the zero-energy modes under the SIBC. The un-normalized solution is given by

$$a_n = \left(-\frac{t_1 - \delta}{t_2} \right)^n, \quad b_n = 0, \quad (10)$$

where a_n and b_n are the field amplitudes at the n th unit cell. If we impose the SIBC, $a_\infty \rightarrow 0$, we conclude that a zero-energy solution is available in the semi-infinite lattice as long as $t_2 > t_1 - \delta$.

Suppose that the SIBC spectrum contains zero energy but the OBC spectrum does not, meaning that the finite system is topologically trivial in the conventional sense. This happens when $t_1 - \delta < t_2 < \sqrt{t_1^2 - \delta^2}$. For example, the numerical parameters in Fig. 4(a) satisfy these conditions. We can truncate the state (10) to use it as a quasi-edge state or stabilize it in the finite lattice under the OBC. Let us start with the former one and prepare an initial wave packet according to Eq. (10) with $n = 1, 2, \dots, N$. We numerically find that it stays almost stationary up to a survival time ($\tau \approx 80$) in the finite lattice [Fig. 4(b)]. Next, we stabilize it by changing the coupling in the forward direction at the right edge as can be seen from Fig. 3(b), which is a perturbative change as all other couplings remain the same. This also changes the topological feature

of the finite system. One can analytically see that this new system has a zero-energy mode exactly given by Eq. (10) with $n = 1, 2, \dots, N$. In this case, a second-order exceptional point at zero energy is formed in the system. To this end, we note that this zero-energy state in the finite lattice is robust against coupling disorder as long as the coupling of the forward direction at the right edge remains zero. This guarantees the existence of the exceptional point.

3. Model III

We finally consider the last specific model depicted in Fig. 1(c). The corresponding non-Hermitian Bloch Hamiltonian is given by Eq. (5) with

$$\begin{aligned} d_x &= t_1 + (t_2 + t_3) \cos k + i\delta \sin k, \\ d_y &= (t_2 - t_3) \sin k + i\delta \cos k, \end{aligned} \quad (11)$$

where t_1 , t_2 , t_3 , and δ are constants [45]. Here, we obtain conclusions similar to those of the other two models. Let us study a particular example without a conventional topological zero mode. Suppose $t_1 = 0.6$, $t_2 = 0.8$, and $t_3 = \delta = 1$. The corresponding PBC spectrum (6) describes two closed loops with the outer one encircling the complex OBC spectrum as can be seen from Fig. 4(c). The corresponding system is topologically trivial in the conventional sense, and the OBC spectrum does not contain zero energy. However the SIBC spectrum contains zero energy. We aim to stabilize the zero-energy mode of the semi-infinite lattice in a finite lattice with open edges. A family of the SIBC zero-energy mode is given by

$$a_n = \frac{(t_1 - \Delta)^n - (t_1 + \Delta)^n}{(-2t_2)^n}, \quad b_n = 0, \quad (12)$$

where $\Delta = \sqrt{t_1^2 - 4t_2(t_3 - \delta)}$ and $a_\infty \rightarrow 0$. Then we prepare an initial wave packet according to Eq. (12) in the finite lattice. We numerically find that $\tau \approx 40$ for the above parameters and $N = 100$ [Fig. 4(d)]. Next, we stabilize it in the finite lattice; i.e., $\tau \rightarrow \infty$ by making a perturbative change in the lattice. Suppose that the coupling between the sites in the last sublattice is zero and the forward coupling between a_{n-1} and a_n is also zero as can be seen from Fig. 3(d). All other couplings remain the same. In this case, the solution (12) with $n = 1, 2, \dots, N$ becomes an exact eigenstate of the finite lattice. It is, in fact, a conventional zero-energy topological mode and the system becomes topologically nontrivial. Furthermore, we also numerically check that an exceptional point is formed in the system; i.e., there exists one state corresponding to the two zero-energy eigenvalues. This zero-energy topological state is also an exceptional state.

IV. CONCLUSION

According to the standard bulk-boundary correspondence, an edge state appears at the interface of a topological insulator with an ordinary insulator. In non-Hermitian tight-binding lattices, the standard bulk-boundary correspondence fails when the PBC and OBC spectra are dramatically different from each other. For the 1D non-Hermitian tight-binding lattices with asymmetric couplings between adjacent sites, the PBC spectrum forms a loop or loops in the complex energy plane,

and the SIBC spectrum fills the interior of the loop or loops. On the other hand, the OBC spectrum is a subset of the SIBC spectrum, implying that an OBC state is also a SIBC state but the reverse is not always true. A skin state that appears only under SIBCs can also be used as a quasi-edge state in the finite lattice with open edges. In this paper, we showed that survival times can be quite long in some systems but reduce dramatically in the presence of noises in the preparation of pure quasi-edge states in the finite lattices. We further discuss how a change in the coupling at the edge of the lattice allows us to stabilize a particular quasi-edge state in the finite lattice. Of special importance is the stabilization of zero-energy quasi-edge states that can be possible by generating

an exceptional point in the chiral symmetric two-band non-Hermitian lattices. In this way, the topological feature of the system can be changed without bang-gap closing and reopening.

ACKNOWLEDGMENTS

C.Y. wishes to acknowledge the support from the Scientific and Technological Research Council of Turkey with Grant No. 1059B191900044. H.R. acknowledges the support by the Army Research Office under Grant No. W911NF-20-1-0276 and the NSF under Grants No. PHY-2012172 and No. OMA-2231387.

-
- [1] H. Shen, B. Zhen, and L. Fu, *Phys. Rev. Lett.* **120**, 146402 (2018).
- [2] H. Jiang, L.-J. Lang, C. Yang, S.-L. Zhu, and S. Chen, *Phys. Rev. B* **100**, 054301 (2019).
- [3] C. Yuce, *Ann. Phys.* **415**, 168098 (2020).
- [4] Y. Liu, Q. Zhou, and S. Chen, *Phys. Rev. B* **104**, 024201 (2021).
- [5] C. Yuce, *Phys. Lett. A* **378**, 2024 (2014).
- [6] J. Claes and T. L. Hughes, *Phys. Rev. B* **103**, L140201 (2021).
- [7] L.-Z. Tang, G.-Q. Zhang, L.-F. Zhang, and D.-W. Zhang, *Phys. Rev. A* **103**, 033325 (2021).
- [8] Q.-B. Zeng and Y. Xu, *Phys. Rev. Res.* **2**, 033052 (2020).
- [9] C. Yuce, *Phys. Lett. A* **408**, 127484 (2021).
- [10] Y. Yi and Z. Yang, *Phys. Rev. Lett.* **125**, 186802 (2020).
- [11] S. Longhi, *Phys. Rev. Lett.* **122**, 237601 (2019).
- [12] S. Schiffer, X.-J. Liu, H. Hu, and J. Wang, *Phys. Rev. A* **103**, L011302 (2021).
- [13] Z. Ozcakmakli Turker and C. Yuce, *Phys. Rev. A* **99**, 022127 (2019).
- [14] C. Yuce, *Phys. Lett. A* **384**, 126094 (2020).
- [15] X. Cai, *Phys. Rev. B* **103**, 014201 (2021).
- [16] T. Li, Y.-S. Zhang, and W. Yi, *Phys. Rev. B* **105**, 125111 (2022).
- [17] C. H. Lee and R. Thomale, *Phys. Rev. B* **99**, 201103(R) (2019).
- [18] Z.-X. Zhang, R. Huang, L. Qi, Y. Xing, Z.-J. Zhang, and H.-F. Wang, *Ann. Phys.* **533**, 2000272 (2020).
- [19] P. Wang, L. Jin, and Z. Song, *Phys. Rev. A* **99**, 062112 (2019).
- [20] M. Ezawa, *Phys. Rev. B* **99**, 121411(R) (2019).
- [21] C. H. Lee, L. Li, and J. Gong, *Phys. Rev. Lett.* **123**, 016805 (2019).
- [22] L. Li, C. H. Lee, S. Mu, and J. Gong, *Nat. Commun.* **11**, 5491 (2020).
- [23] F. K. Kunst, G. van Miert, and E. J. Bergholtz, *Phys. Rev. B* **99**, 085427 (2019).
- [24] C. Yuce, *Phys. Rev. A* **102**, 032203 (2020).
- [25] H. Jiang, R. Lü, and S. Chen, *Eur. Phys. J. B* **93**, 125 (2020).
- [26] J. Y. Lee, J. Ahn, H. Zhou, and A. Vishwanath, *Phys. Rev. Lett.* **123**, 206404 (2019).
- [27] Y. Cao, Y. Li, and X. Yang, *Phys. Rev. B* **103**, 075126 (2021).
- [28] C. Yuce, *Phys. Lett. A* **379**, 1213 (2015).
- [29] C. Yuce, *Phys. Rev. A* **99**, 032109 (2019).
- [30] J. Zhong, K. Wang, Y. Park, V. Asadchy, C. C. Wojcik, A. Dutt, and S. Fan, *Phys. Rev. B* **104**, 125416 (2021).
- [31] K.-I. Imura and Y. Takane, *Phys. Rev. B* **100**, 165430 (2019).
- [32] N. Okuma, K. Kawabata, K. Shiozaki, and M. Sato, *Phys. Rev. Lett.* **124**, 086801 (2020).
- [33] K. Zhang, Z. Yang, and C. Fang, *Phys. Rev. Lett.* **125**, 126402 (2020).
- [34] Z. Yang, K. Zhang, C. Fang, and J. Hu, *Phys. Rev. Lett.* **125**, 226402 (2020).
- [35] K. Wang, A. Dutt, K. Y. Yang, C. C. Wojcik, J. Vuckovic, and S. Fan, *Science* **371**, 1240 (2021).
- [36] S. Yao, F. Song, and Z. Wang, *Phys. Rev. Lett.* **121**, 136802 (2018).
- [37] S. Yao and Z. Wang, *Phys. Rev. Lett.* **121**, 086803 (2018).
- [38] Z. Gong, Y. Ashida, K. Kawabata, K. Takasan, S. Higashikawa, and M. Ueda, *Phys. Rev. X* **8**, 031079 (2018).
- [39] C. Yuce, *Phys. Lett. A* **403**, 127384 (2021).
- [40] S. Longhi, *Opt. Lett.* **46**, 6107 (2021).
- [41] S. Longhi, *Proc. R. Soc. A* **478**, 20210927 (2022).
- [42] N. Hatano and D. R. Nelson, *Phys. Rev. Lett.* **77**, 570 (1996).
- [43] S. Weidemann, M. Kremer, T. Helbig, T. Hofmann, A. Stegmaier, M. Greiter, R. Thomale, and A. Szameit, *Science* **368**, 311 (2020).
- [44] K. Yokomizo and S. Murakami, *Phys. Rev. Lett.* **123**, 066404 (2019).
- [45] S. Longhi, *Phys. Rev. Res.* **1**, 023013 (2019).